Published in final edited form as:
Semin Radiat Oncol. 2010 July ; 20(3): 156–163. doi:10.1016/j.semradonc.2010.01.003.

The Tumor Microenvironment in Non-Small Cell Lung Cancer

Edward E. Graves, Ph.D.[1], **Amit Maity, M.D., Ph.D**[2], and **Quynh-Thu Le, M.D.**[3]
[1] Assistant Professor, Dept. of Radiation Oncology, Stanford University School of Medicine, Stanford, CA

Abstract

The tumor microenvironment (TME) of NSCLC is heterogeneous with variable blood flow though leaky immature vessels, resulting in regions of acidosis and hypoxia. Hypoxia has been documented in NSCLC directly by polarographic needle electrodes and indirectly by assessing tissue and plasma hypoxia markers. In general, elevated expression of these markers portends poorer outcomes in NSCLC. Impaired vascularity and hypoxia can lead to increased metastasis and treatment resistance. Compounds that directly target hypoxic cells such as tirapazamine have been tested in clinical trials for NSCLC with mixed results. Pre-clinical data, however, suggest other ways of exploiting the abnormal TME in NSCLC for therapeutic gain. Inhibition of HIF-1α or VEGF may increase local control after radiation. Inhibitors of the EGFR/PI3K/Akt pathway such as erlotinib or PI-103 may “normalize” tumor vessels, allowing for increased chemotherapy delivery or improved oxygenation and radiation response. In order to select patients who may respond to these therapies and to evaluate the effects of these agents, a non-invasive means of imaging the TME is critical. Presently, there are several promising modalities to image hypoxia and the tumor vasculature; these include dynamic perfusion imaging and positron emission tomography (PET) scanning with radiolabled nitroimidazoles.

Introduction

The microenviroment of solid tumors is complex. Surrounding cancer cells are the cells forming the stroma, microvasculature, lymphatics and immune response.[1] Depending on the composition of these “stromal cells” and the local cytokine milieu, the level of tumor oxygenation, nutrients, pH and interstitial pressure can be highly variable within the same tumor. Recent data have shown that the tumor microenvironment (TME) plays an important role in both malignant tumor progression and treatment response.[1] Since most published data on lung cancers concentrate on tumor vasculature and oxygenation and little is known about other components of the TME, we will focus this review on the first two components.

[2]Corresponding author: Associate Professor, Dept. of Radiation Oncology, University of Pennsylvania School of Medicine, 195 John Morgan Bldg., 3620 Hamilton Walk, Philadelphia, PA 19104, Phone: (215) 614-0078, Fax: (215) 898-0090, maity@uphs.upenn.edu.
[3]Corresponding author: Professor and Clinical Research Director, Dept. of Radiation Oncology, Stanford University School of Medicine, 875 Blake Wilbur Dr, MC 5847, Stanford, CA, 94305–5847, Phone: (650) 498–5032, Fax: (650) 725–8231, qle@stanford.edu

Financial disclosures: Q-T L received research funding from Glaxo-Smith Kline, Amgen and Varian for investigator initiated studies, unrelated to the discussed topics.

Significance of hypoxia in lung cancers

Hypoxia, or the condition of low oxygen, is a common phenomenon in solid neoplasms. It arises when tissue oxygen demands exceed oxygen supplies, due to aberrant blood vessel formation, fluctuations in blood flow and increasing oxygen demands from rapid tumor expansion.[2] Since the recognition of tumoral hypoxia in 1955,[3] it has been shown to limit tumor cells' response to therapy and predispose them towards metastasis. Mechanistically, tumor hypoxia mediates tumor progression by selecting cells with diminished apoptotic potential and activating genes involved in angiogenesis, metastasis and metabolism.[4–6]

Presently, there are several methods for detecting tumor hypoxia but none represents a clear "gold standard".[7] The lack of an ideal hypoxia detection strategy is due to the complex nature of blood supplies and cellular oxygen consumption, giving rise to extreme spatial and temporal heterogeneities in tumor oxygen levels. None of the current methods can completely capture such heterogeneity. With regards to human lung cancers, the clinical data on hypoxia are quite meager. Although many approaches have been used to study hypoxia in superficially located tumors such as cervical or head and neck cancers, only three methods have been employed to assess hypoxia in lung cancers. These approaches are (1) measurement of partial oxygen pressure (pO_2) with needle electrodes, (2) detection of hypoxia-induced proteins in tumor or blood, (3) and imaging hypoxia and tumor vasculature.

Our group performed the only published study on *in vivo* tumor pO_2 measurement in human non-small cell lung cancers (NSCLC).[8] Since these tumors are deeply situated, such an approach can only be executed intraoperatively during surgical resection of the primary tumor. Twenty patients with resectable NSCLC were enrolled, and measurements of deflated normal lung and tumor pO_2 were performed with the polarographic electrode (pO_2 histograph, Eppendorf, Hamburg, Germany). We measured levels of plasma osteopontin (OPN), a secreted hypoxia-induced protein, and performed immunohistochemical (IHC) staining of tumor tissue for carbonic anhydrase-IX (CAIX), a hypoxia-induced membrane protein. We also performed gene expression profiling of fresh tumor tissues in 12 patients. We found that the tumor pO_2 was lower than the lung pO_2 in all but one patient. The ratio of tumor to normal lung (T/L) pO_2 significantly correlated with plasma OPN levels ($r = 0.53$, $p = 0.02$) and CAIX expression ($p = 0.006$). Gene expression profiling showed that high CD44 expression, a known cell surface receptor for OPN, was a predictor for relapse, which was confirmed by tissue staining of CD44v6 protein. Other parameters associated with the risk of relapse were T-stage ($p = 0.02$), T/L pO_2 ($p = 0.04$) and OPN levels ($p = 0.001$). Overall, our study found that tumor hypoxia does exist in resectable NSCLC and correlated with poor prognosis. Such results, although intriguing, will need to be validated in larger studies.

In contrast to the small microelectrode study, there is a wealth of information on the relationship between treatment outcomes and the expression of certain hypoxia-regulated proteins, including the hypoxia inducible factor-1 (HIF-1), which regulates genes involved in metabolism, angiogenesis, invasion and metastasis [9] and some of its targets such as glucose transporter 1 (Glut-1) and CAIX. The results from representative large series (>40 patients) are summarized in Table 1. These data demonstrate that elevated expression of hypoxia markers, in general, portends poorer prognosis in patients treated with either surgical or non-surgical therapies. Interestingly, total protein expression of hypoxia markers may not tell the entire story. A recent study of 158 resected NSCLC found that CAIX staining in the stromal fibroblasts was more prognostic for survival than CAIX staining in adjacent tumor cells.[10] These findings suggest the need to differentiate the contribution of stromal from tumor hypoxia.

Other hypoxia regulated proteins that have been studied in other solid cancers are VEGF, BNIP3 (Bcl-2/adenovirus E1B 19 kDA-interacting enzyme), Lysyl oxidase (LOX), Lactate Dehydrogenase isoenzyme-5 (LDH-5), Plasminogen activator inhibitor-1 (PAI-1) and Galectin-1.[11–17] The clinical relevance of these proteins in lung cancer has not yet been explored.

Under hypoxic stress, tumor and surrounding stromal cells secrete proteins that can be detected in the circulation. Known circulating markers for hypoxia include VEGF and OPN. A systematic review of published studies indicated that VEGF overexpression was associated with a poor prognosis in both NSCLC and small cell lung cancers.[18] Our group has previously identified OPN as a secreted hypoxia marker in head and neck cancer.[19] We have also shown that circulating OPN levels correlated with tumor pO_2 in 20 NSCLC patients (see above).[8] More importantly, expression of OPN and its receptor, CD44v6, correlated with survival in these patients. We subsequently evaluated OPN levels in 172 patients with metastatic NSCLC treated with chemotherapy in a cooperative group study.[20] Higher circulating OPN level was an independent prognostic factor for survival.

Targeting hypoxia in NSCLC

Taken together, the above data suggest that hypoxia exists at a certain level in lung cancers and may influence prognosis. The question is whether one can target hypoxia in these tumors. Since the 1950s, several strategies have been used to overcome tumor hypoxia. These include hyperbaric oxygen treatment [21], the use of drugs to reduce oxygen binding to hemoglobin (e.g. RSR13),[22] the use of vasodilators and carbogen (ARCON) to enhance oxygen tissue delivery,[23] the use of electron affinity drugs as hypoxic cell radiosensitizers,[24] and treatment with high linear-energy transfer (LET) radiation whose cytotoxic effect is less dependent on oxygen.[25] Although these strategies have not achieved general acceptance, a meta-analysis of trials using hypoxic cell sensitizers or hyperbaric oxygen showed a small but significant benefit for locoregional control and survival.[21]

The latest strategy incorporates drugs that can directly kill hypoxic cells, and the prototype is tirapazamine (TPZ). TPZ has been extensively studied in combination with chemotherapy with mixed results in metastatic NSCLC patients.[26–29] While an initial randomized study suggested that the addition of TPZ to cisplatin was superior to cisplatin alone,[27] additional randomized studies found that either replacing etoposide with TPZ or adding TPZ to a platinum-doublet was not superior to the control arms.[28, 29] None of these studies tested TPZ in combination with concurrent radiation and chemotherapy. Interestingly, the Southwest Oncology group performed a pilot study (S0004) combining TPZ with thoracic radiation, cisplatin, and etoposide in patients with limited stage small cell lung cancer (LSCLC).[30] The median survival of 22 months in this pilot study exceeded those noted for prior SWOG studies in this setting. These results prompted a phase II validation study (S0222), which accrued 69 patients. S0222 replicated the promising median survival of S0004.[31] These intriguing findings suggested that hypoxia-targeted therapies should be further studied in LSCLC.

Another potential scenario for targeting hypoxia in lung cancers is in the setting of stereotactic body radiation therapy (SBRT). Radiobiological modeling suggests that hypoxia would have a greater impact on the efficacy of a single large fraction than on fractionated treatment because of the lack of reoxygenation in the former. While this has been known for decades, the field of stereotactic radiotherapy has been thriving, first for brain tumors and subsequently for extracranial sites. Although early local control rates for lung cancer SBRT have been excellent, longer follow up suggests that the results are poorer for larger tumors, where one would expect more hypoxia.[32]

Bauman *et al.* reported that most of their local failures were in tumors with higher T-stage or larger GTV.[33] In another phase II study, the 3-year local control rate after SBRT was 78% for T1 tumors and 40% for T2 tumors.[34] For CNS metastases, lesions with central necrosis had a poorer local control rate than non-necrotic lesions after single fraction treatment.[35] These data suggested that the influence of hypoxia on local control should be investigated for lung cancer SBRT. In the ideal situation, hypoxia imaging can be performed prior to SBRT and correlated with local control in NSCLC. If hypoxia imaging predicts for local failure, then it can be used to guide patient selection for dose escalation, modification of fractionation, or for concomitant treatment with hypoxic cell radiosensitizer. Since SBRT involves treating the entire target to an ablative dose, the presence of hypoxia is more relevant than its spatial and temporal fluctuation, making hypoxia imaging more applicable in this setting.

Imaging the microenvironment of lung cancer

As described above, detection and measurement of the TME using noninvasive imaging is a potential clinical avenue towards TME-specific patient staging and treatment. The advent of molecular imaging has seen modalities such as positron emission tomography (PET), single photon emission computed tomography (SPECT), magnetic resonance spectroscopy (MRS), and optical imaging develop from laboratory research tools into established clinical procedures. By detecting, quantifying, and localizing specific molecular signals, either through direct detection of endogenous components or through observation of exogenously delivered molecular probes, it is now possible to noninvasively measure a variety of functional aspects of tissue, including expression of specific genes and proteins, metabolism, perfusion, hypoxia, and cellular proliferation. While imaging of glucose metabolism using positron emission tomography (PET) and the radiotracer [^{18}F]-fluorodeoxyglucose (FDG) is the most well developed molecular imaging method for lung cancer, a number of emerging techniques focused on assessment of specific aspects of the TME have been applied towards lung cancer in human patients.

Perfusion and Angiogenesis Imaging

In general, imaging of tumor perfusion and angiogenesis can be classified into two categories: 1) measurement of blood flow and vessel permeability using dynamic imaging over the course of contrast agent passage through the vasculature, and 2) imaging of molecular components of angiogenic and/or tumor-associated blood vessels. The former approach has been applied with imaging modalities including x-ray CT, magnetic resonance imaging, ultrasound, positron emission tomography, and single photon emission computed tomography, using contrast materials appropriate to each. This method is generically called dynamic contrast-enhanced imaging, and involves bolus injection of a contrast material and imaging at regular timepoints before and during passage of the bolus through the vasculature. The acquired imaging time course is then analyzed on a pixel-by-pixel or region-by-region basis, either by direct analysis of the time-uptake curve to quantify parameters such as time to peak uptake, maximum uptake, and peak slope, or through fitting of the time-uptake curve in order to generate parametric images of the fitting parameters, which typically include some combination of vascular volume, perfusion, and vessel permeability.[36, 37] The schedule of image acquisitions over contrast delivery as well as the quantitative models used in the fitting process are not standardized and are topics of current research and development. In the lung, this procedure is complicated by the need to compensate for respiratory motion over the course of the acquisition, however breath hold and/or respiratory gating schemes have been applied to investigate perfusion imaging of lung tumors.[38, 39]

Dynamic x-ray computed tomography and magnetic resonance imaging studies before and after contrast delivery have been applied extensively to investigate vascularity of lung lesions. Acquisition protocols typically include imaging at periods of 2 – 20 seconds per image over 2 – 10 minutes post-injection. Using perfusion CT following iodinated contrast delivery, greater peak enhancement has been noted for malignant and inflammatory lesions than for benign lesions.[40, 41] Dynamic MRI studies have noted that malignant lung lesions are associated with a stronger peak contrast enhancement, a faster contrast arrival, and a significant contrast washout relative to benign lesions, suggesting malignant tumors are well vascularized.[38, 42] Recent studies fitting dynamic MRI data to compartmental models have demonstrated the ability of this technique to resolve intratumoral variations in perfusion and vascular permeability.[39]

Detection of the molecular characteristics of tumor angiogenesis is an emerging application of molecular imaging for lung lesions. At present the most well-developed angiogenesis probes used for molecular imaging are peptides bearing the arginine-glycine-aspartic acid (RGD) motif. These peptides have been shown to bind to α_V-β_3 integrins expressed preferentially on tumor-associated vasculature.[43, 44] A variety of RGD peptides have been labeled for imaging applications, and several of these have entered early clinical trials. PET imaging of [^{18}F]-galacto-RGD in ten patients with primary and metastatic NSCLC has revealed mean standardized uptake values (SUVs) between 0.3 and 5.8, with no correlation to FDG uptake, suggesting that this modality provides unique information.[45] Preclinical studies of RGD imaging agents have demonstrated the ability of this probe to monitor changes in tumor vascularity following therapy in xenograft models of lung cancer.[46]

Hypoxia Imaging

Several types of molecules have demonstrated specific accumulation in hypoxic cells, notably the 2-nitroimidazoles. These molecules are reduced by a set of intracellular reductases, which cause them to become reactive and covalently bind to intracellular macromolecules. This reduction and trapping can be reversed by molecular oxygen, resulting in the accumulation of 2-nitroimidazoles only in hypoxic cells. Several compounds of this type, including pimonidazole and 2-(2-Nitro-1-H-imidazol-1-yl)-N-(2,2,3,3,3-pentafluoropropyl) acetamide (EF5), have been used as immunohistochemical markers of hypoxia after visualization with specific antibodies.[47, 48] Radioisotopes have been conjugated to these molecules, producing hypoxia-specific radiotracers for nuclear medicine. Agents of this class include [^{18}F]-Fluoromisonidazole (FMISO),[49] [^{18}F]-Fluoroazomycin arabinoside (FAZA),[50] and [^{18}F]-EF5 (EF5).[51] Another notable hypoxia-specific radiotracer is [Cu]-Diacetyl-bis(N4-methylthiosemicarbazone) (Cu-ATSM, half life ^{60}Cu: 23.7 minutes, ^{62}Cu: 9.7 minutes, ^{64}Cu: 12.7 hours), which functions through reduction of the copper atom to produce a charged and membrane-impermeable form of the probe.[52] Analogous development of hypoxia imaging radiotracers for SPECT has resulted in a number of 2-nitroimidazole-based agents [53] as well as HL-91, a probe based on the same core ligand design but lacking the nitroimidazole group.[54]

Using a tumor:blood FMISO ratio of 1.4 as a cutoff for hypoxic voxels within a lesion, fractional hypoxic volumes (FHV = volume of FMISO-identified hypoxic regions divided by the total tumor volume) between 1.3 and 94.7% were observed for 21 non-small cell lung tumors (median 47.6%).[55] Maximum SUVs between 0.40 and 2.14 (tumor:normal lung ratios between 1.18 and 9.73) were reported for 17 NSCLC patients.[56] Although key components of FDG uptake including glucose transporter 1 and hexokinase are regulated by hypoxia and HIF-1, no correlation between FMISO and FDG uptake was observed in this patient sample. [^{60}Cu]-ATSM has also been applied towards the study of lung cancer, demonstrating greater maximum SUVs than FMISO (1.5 to 4.7) but similar

tumor:background ratios (1.2 to 4.8) in a sample of 18 NSCLC patients.[57] Interestingly, in this cohort uptake of [^{60}Cu]-ATSM was significantly lower in patients who responded to therapy (either radiation, chemotherapy, or a combination of both) than in those who did not (1.5 versus 3.4).

Changes in FHV measured by FMISO PET before and after fractionated radiotherapy have been reported for a preliminary cohort of 7 NSCLC patients, revealing a general downward trend in FHV over a 6 week course of fractionated radiotherapy.[58] A preliminary study of FMISO and FDG PET in 8 NSCLC patients before and after chemoradiotherapy demonstrated 20–30% reductions in uptake of both radiotracers 14 days after the conclusion of chemotherapy. The parallel findings observed with FDG and FMISO as well as the relatively coarse spatial resolution of PET imaging (~5 mm for clinical scanners) raises the question of whether differential changes in FMISO or other functional imaging signals reflect changes in their specific molecular targets or simply changes in tumor volume and/or cellularity. Future studies of molecular imaging combining emerging and established methods will be required to resolve this dilemma.

Altering the TME to increase radiation response

As discussed above, efforts to target hypoxia in patients with NSCLC have not been a stunning success, but there is still interest in modulating the TME to improve therapy. There is a clear relationship between hypoxia and radioresistance. Hypoxic cells require 2–3-fold higher radiation dose as do well-oxygenated cells to achieve the same level of killing due to the fact that oxygen is required to generate free radicals to elicit maximal DNA damage.[59] Other factors in the TME that may influence radiation response include the radiosensitivity of the surrounding stromal cells and intratumoral expression of factors such as VEGF and HIF-1α. Several classes of agents can modulate the TME in preclinical models.

HIF-1 and VEGF as targets for radiosensitization

A potential target that could influence radiosensitivity is HIF-1, which as discussed previously is a master transcription factor activated in response to hypoxia. Agents that target HIF-1, such as YC-1 and PX-478, can increase the radioresponsiveness of tumors.[60, 61] Zeng *et al*. showed that the HIF-1 inhibitor TS-1 enhanced the therapeutic effect of a single dose of 14 Gy and further delayed tumor regrowth of H441 NSCLC xenografts.[62]

The HIF-1 target VEGF is a potent mediator of angiogenesis that enhances endothelial cell survival, induces vasodilatation, and regulates pericyte coverage.[63] However, VEGF also increases vascular permeability.[64] Perhaps because supraphysiologic VEGF secretion causes excessive leakiness or because of a lack of coordinate expression of other angiogenic factors, the vessels within a tumor appear dilated, saccular, and tortuous and function poorly with sluggish blood flow. Therefore, despite high VEGF expression, which should act as a compensatory mechanism, tumors often remain hypoxic.

Gorski *et al*. found that VEGF was induced after irradiation both *in vitro* and *in vivo* in Lewis lung carcinomas (LLC).[65] Treatment of mice bearing LLC xenografts with an anti-VEGF antibody prior to irradiation synergistically inhibited regrowth. Williams *et al*. showed that the combination of radiation and cediranib (RECENTIN, AZD2171), a highly potent inhibitor of VEGFR1, 2, and 3, significantly increased growth delay of Calu-6 NSCLC xenografts compared with either modality alone.[66] They showed that the drug had to be given concomitantly with radiation or immediately following radiation to see a synergistic effect.[66] They also showed that the combination of radiation and ZD6474, a dual VEGF and epidermal growth factor receptor (EGFR) inhibitor, had a greater effect on delaying Calu-6 xenograft regrowth than either treatment alone.[67]

Several mechanisms have been proposed to explain how anti-HIF or anti-VEGF therapy might increase tumor control following radiation including (i) radiosensitization of the endothelial cells and (ii) blunting of the stromal response to prevent the establishment of new vasculature following radiation. Another potential mechanism is by vascular normalization. This concept, first proposed by Rakesh Jain, hypothesizes that high intratumoral VEGF expression actually reduces tumor oxygenation because the vessels function poorly.[68] Paradoxically, inhibition of VEGF expression in these tumors may cause the vessels to remodel, becoming less permeable and less aberrant and resulting in decreased interstitial fluid pressure (IPF), improved blood flow and increased tumor oxygenation. Pre-clinical data supporting this idea exist.[69] However, it remains to be seen whether vascular normalization is a general phenomenon that occurs in patients with a variety of cancers receiving anti-HIF/VEGF therapy and whether this leads to improved oxygenation that contributes to increased radiosensitivity. A review of the literature on the effects on anti-angiogenic agents on tumor oxygenation shows this issue to be very complicated, with some drugs increasing hypoxia and others decreasing it.[70]

Epidermal growth factor receptor (EGFR) inhibitors

The EGFR receptor (erb1/EGFR), a member of the family of receptor tyrosine kinases, is overexpressed in 80% of NSCLC and mutated in a smaller percentage. EGFR activation leads to the activation of multiple intracellular signaling pathway including the Ras and Akt pathways. EGFR inhibitors including the monoclonal antibody cetuximab (Erbitux, Imclone, New York, NY) and the small molecule tyrosine kinase inhibitors gefitinib (Iressa, AstraZeneca, London, England) and erlotinib (Tarceva, OSI Pharmaceuticals, Melville, NY) have been used in the clinic.

Preclinical evidence indicates that EGFR inhibition can increase radiosensitivity in NSCLC cell lines as reviewed previously.[71] In mice bearing EGFR-expressing, NSCLC xenografts, cetuximab plus radiation markedly improved tumor growth inhibition over either agent alone.[72] Similarly, Harari's group showed that erlotinib and radiation act synergistically to inhibit tumor regrowth of H226 NSCLC xenografts.[73] Results of clinical trials using EGFR inhibitors with radiation in NSCLC are not available; however, for locally advanced head and neck squamous cell carcinoma (HNSCC), cetuximab and radiation led to increased survival and local control over radiation alone in a randomized phase III trial.[74]

We have investigated the effects of EGFR inhibition on the TME based on our previous work showing that the EGFR inhibitors erlotinib and gefitinib decreased VEGF mRNA and protein expression.[75] More recently we have shown that erlotinib treatment altered vessel morphology and decreased vessel permeability within HNSCC xenografts grown in nude mice.[76] Furthermore, erlotinib increased tumor blood flow and decreased hypoxia. Similar increased blood flow was seen in mice bearing H226 NSCLC xenografts treated with erlotinib. We hypothesize that these changes in tumor physiology are an indirect effect of EGFR inhibition causing decreased VEGF secretion by the tumor cells, leading to vascular normalization, improved blood flow, and improved oxygenation.

The Phosphatidylinositol 3-kinase (PI3K)/Akt pathway

The PI3K pathway, which plays a key role in controlling cell proliferation, growth and survival, is activated in many cancers.[77] PI3K phosphorylates the 3′-OH of the inositol ring of phosphatidylinositol, leading to phosphatidylinositol 3,4,5-trisphosphate (PIP3) synthesis. PIP3 binds the serine/threonine kinase Akt and allows it be phosphorylated. The phosphatase and tensin homologue gene (PTEN) phosphatase opposes the action of PI3K, thereby reducing the level of activated (phosphorylated) Akt. The frequency of P-Akt activation in NSCLC ranges between 50–83%.[78, 79]

Activation of the PI3K/Akt pathway has been associated with radioresistance in many cell types.[80] Gupta *et al.* showed that three NSCLC cell lines with high P-Akt levels were radiosensitized *in vitro* using the inhibitor LY294002.[78] However, LY294002, and the other commonly used PI3K inhibitor wortmannin, are too toxic for human use. Hence, pharmaceutical companies have been actively developing PI3K inhibitors. Prevo *et al*. found that PI-103, a pyridinylfuranopyrimidine compound, enhanced radiation sensitivity of tumor cells *in vitro* and led to persistence of DNA damage.[81] The same group showed that the drug caused *in vivo* changes in the vessel morphology in xenografts grown in nude mice consistent with vascular normalization.[82] This was accompanied by increased blood flow and decreased tumor hypoxia.

Our group and others have demonstrated that HIV protease inhibitors (HPIs) such as nelfinavir (Viracept, Agouron Pharmaceuticals, La Jolla, CA) interfere with PI3K-Akt signaling and radiosensitize a variety of tumor types.[83, 84] The effect of nelfinavir often appears greater *in vivo* than *in vitro*, leading us to hypothesize that the drug might have additional effects on the TME. Nelfinavir decreases HIF-1α and VEGF expression both *in vitro* and *in vivo*, and it improves tumor oxygenation in A549 lung carcinoma xenografts.[85] Nelfinavir can also increase blood flow in tumors (Cerniglia and Maity; unpublished observations). Thus, our results with nelfinavir are very similar to those with erlotinib.[76] We hypothesize that both nelfinavir and erlotinib decrease VEGF secretion by tumor cells, resulting in vascular normalization. Supporting this idea, Qayum *et al.* found that nelfinavir treatment resulted in vessel changes that are consistent with normalization.[82]

Conclusion

The microenvironment of lung cancers is heterogeneous and plays an important role in determining outcome. For example, hypoxia is associated with increased risk of metastases as well as resistance to radiation therapy and perhaps chemotherapy as well. The altered vasculature seen in lung cancers contributes to hypoxia and makes it difficult to efficiently deliver agents through the bloodstream. The TME poses a challenge for therapy but also presents an opportunity. We now have a variety of clinically applicable agents that can modulate the TME in a way that might improve response to subsequent cytotoxic therapy. However, most of this work has been performed in animal models. There is a paucity of clinical data from patients showing that alteration of the TME is an important mechanism by which biological agents can sensitize tumors to radiation or chemotherapy. However, as discussed in this review, we do have the clinical tools available to assess aspects of the TME including tumor oxygenation and vascularity, using both radiologic imaging and biomarkers.

Acknowledgments

This work was supported by NIH R01 CA093638 (A.M.), NIH R01 CA131199 (E. G.) and NIH PO1 CA67166 (Q-T. L.)

References

1. Joyce JA, Pollard JW. Microenvironmental regulation of metastasis. Nat Rev Cancer 2009;9:239–52. [PubMed: 19279573]
2. Brown JM, Giaccia AJ. The unique physiology of solid tumors: opportunities (and problems) for cancer therapy. Cancer Res 1998;58:1408–16. [PubMed: 9537241]
3. Thomlinson RH, Gray LH. The histological structure of some human lung cancers and the possible implications for radiotherapy. Br J Cancer 1955;9:539–549. [PubMed: 13304213]
4. Graeber TG, Peterson JF, Tsai M, et al. Hypoxia induces the accumulation of p53 protein, but the activation of a G1-phase checkpoint by low oxygen conditions is independent of p53 status. Mol Cell Biol 1994;14:6264–6277. [PubMed: 8065358]

5. Le QT, Denko NC, Giaccia AJ. Hypoxic gene expression and metastasis. Cancer Metastasis Rev 2004;23:293–310. [PubMed: 15197330]

6. Papandreou I, Cairns RA, Fontana L, et al. HIF-1 mediates adaptation to hypoxia by actively downregulating mitochondrial oxygen consumption. Cell Metab 2006;3:187–97. [PubMed: 16517406]

7. Tatum JL, Kelloff GJ, Gillies RJ, et al. Hypoxia: importance in tumor biology, noninvasive measurement by imaging, and value of its measurement in the management of cancer therapy. Int J Radiat Biol 2006;82:699–757. [PubMed: 17118889]

8. Le QT, Chen E, Salim A, et al. An evaluation of tumor oxygenation and gene expression in patients with early stage non-small cell lung cancers. Clin Cancer Res 2006;12:1507–14. [PubMed: 16533775]

9. Giaccia A, Siim BG, Johnson RS. HIF-1 as a target for drug development. Nat Rev Drug Discov 2003;2:803–11. [PubMed: 14526383]

10. Nakao M, Ishii G, Nagai K, et al. Prognostic significance of carbonic anhydrase IX expression by cancer-associated fibroblasts in lung adenocarcinoma. Cancer 2009;115:2732–43. [PubMed: 19365853]

11. Le QT, Shi G, Cao H, et al. Galectin-1: a link between tumor hypoxia and tumor immune privilege. J Clin Oncol 2005;23:8932–41. [PubMed: 16219933]

12. Le QT, Kong C, Lavori PW, et al. Expression and Prognostic Significance of a Panel of Tissue Hypoxia Markers in Head-and-Neck Squamous Cell Carcinomas. Int J Radiat Oncol Biol Phys 2007;69:167–75. [PubMed: 17707270]

13. Erler JT, Bennewith KL, Nicolau M, et al. Lysyl oxidase is essential for hypoxia-induced metastasis. Nature 2006;440:1222–6. [PubMed: 16642001]

14. Koukourakis MI, Giatromanolaki A, Sivridis E, et al. Lactate dehydrogenase 5 expression in operable colorectal cancer: strong association with survival and activated vascular endothelial growth factor pathway--a report of the Tumour Angiogenesis Research Group. J Clin Oncol 2006;24:4301–8. [PubMed: 16896001]

15. Giatromanolaki A, Koukourakis MI, Sowter HM, et al. BNIP3 expression is linked with hypoxia-regulated protein expression and with poor prognosis in non-small cell lung cancer. Clin Cancer Res 2004;10:5566–71. [PubMed: 15328198]

16. de Witte JH, Sweep CG, Klijn JG, et al. Prognostic impact of urokinase-type plasminogen activator (uPA) and its inhibitor (PAI-1) in cytosols and pellet extracts derived from 892 breast cancer patients. Br J Cancer 1999;79:1190–8. [PubMed: 10098758]

17. Linderholm BK, Lindh B, Beckman L, et al. Prognostic correlation of basic fibroblast growth factor and vascular endothelial growth factor in 1307 primary breast cancers. Clin Breast Cancer 2003;4:340–7. [PubMed: 14715109]

18. Zhan P, Wang J, Lv XJ, et al. Prognostic value of vascular endothelial growth factor expression in patients with lung cancer: a systematic review with meta-analysis. J Thorac Oncol 2009;4:1094–103. [PubMed: 19687765]

19. Le QT, Sutphin PD, Raychaudhuri S, et al. Identification of osteopontin as a prognostic plasma marker for head and neck squamous cell carcinomas. Clin Cancer Res 2003;9:59–67. [PubMed: 12538452]

20. Mack PC, Redman MW, Chansky K, et al. Lower osteopontin plasma levels are associated with superior outcomes in advanced non-small-cell lung cancer patients receiving platinum-based chemotherapy: SWOG Study S0003. J Clin Oncol 2008;26:4771–6. [PubMed: 18779603]

21. Overgaard J, Horsman MR. Modification of Hypoxia-Induced Radioresistance in Tumors by the Use of Oxygen and Sensitizers. Semin Radiat Oncol 1996;6:10–21. [PubMed: 10717158]

22. Shaw E, Scott C, Suh J, et al. RSR13 plus cranial radiation therapy in patients with brain metastases: comparison with the Radiation Therapy Oncology Group Recursive Partitioning Analysis Brain Metastases Database. J Clin Oncol 2003;21:2364–71. [PubMed: 12805339]

23. Kaanders JH, Pop LA, Marres HA, et al. ARCON: experience in 215 patients with advanced head-and-neck cancer. Int J Radiat Oncol Biol Phys 2002;52:769–78. [PubMed: 11849800]

24. Overgaard J, Hansen HS, Overgaard M, et al. A randomized double-blind phase III study of nimorazole as a hypoxic radiosensitizer of primary radiotherapy in supraglottic larynx and pharynx

carcinoma. Results of the Danish Head and Neck Cancer Study (DAHANCA) Protocol 5–85. Radiother Oncol 1998;46:135–46. [PubMed: 9510041]

25. Britten RA, Peters LJ, Murray D. Biological factors influencing the RBE of neutrons: implications for their past, present and future use in radiotherapy. Radiat Res 2001;156:125–35. [PubMed: 11448233]
26. Treat J, Johnson E, Langer C, et al. Tirapazamine with cisplatin in patients with advanced non-small cell lung cancer: a phase II study. J Clin Oncol 1998;16:3524–3527. [PubMed: 9817270]
27. von Pawel J, von Roemeling R, Gatzemeier U, et al. Tirapazamine plus cisplatin versus cisplatin in advanced non-small-cell lung cancer: A report of the international CATAPULT I study group. Cisplatin and Tirapazamine in Subjects with Advanced Previously Untreated Non-Small-Cell Lung Tumors. J Clin Oncol 2000;18:1351–9. [PubMed: 10715308]
28. Shepherd F, Koschel G, von Pawel J, et al. Comparison of Tirazone (Tirapazamine) and cisplatin vs. etoposide and cisplatin in advanced non-small cell lung cancer (NSCLC): Final results of the international phase III CATAPULT II Trial. Lung Cancer 2000;29(S1):28.
29. Williamson SK, Crowley JJ, Lara PN Jr, et al. Phase III trial of paclitaxel plus carboplatin with or without tirapazamine in advanced non-small-cell lung cancer: Southwest Oncology Group Trial S0003. J Clin Oncol 2005;23:9097–104. [PubMed: 16361616]
30. Le QT, McCoy J, Williamson S, et al. Phase I study of tirapazamine plus cisplatin/etoposide and concurrent thoracic radiotherapy in limited-stage small cell lung cancer (S0004): a Southwest Oncology Group study. Clin Cancer Res 2004;10:5418–24. [PubMed: 15328179]
31. Le QT, Moon J, Redman M, et al. Phase II study of tirapazamine, cisplatin, and etoposide and concurrent thoracic radiotherapy for limited-stage small-cell lung cancer: SWOG 0222. J Clin Oncol 2009;27:3014–9. [PubMed: 19364954]
32. Nehmeh SA, Lee NY, Schroder H, et al. Reproducibility of intratumor distribution of (18)F-fluoromisonidazole in head and neck cancer. Int J Radiat Oncol Biol Phys 2008;70:235–42. [PubMed: 18086391]
33. Baumann P, Nyman J, Lax I, et al. Factors important for efficacy of stereotactic body radiotherapy of medically inoperable stage I lung cancer. A retrospective analysis of patients treated in the Nordic countries. Acta Oncol 2006;45:787–95. [PubMed: 16982541]
34. Koto M, Takai Y, Ogawa Y, et al. A phase II study on stereotactic body radiotherapy for stage I non-small cell lung cancer. Radiother Oncol 2007;85:429–34. [PubMed: 18022720]
35. Goodman KA, Sneed PK, McDermott MW, et al. Relationship between pattern of enhancement and local control of brain metastases after radiosurgery. Int J Radiat Oncol Biol Phys 2001;50:139–46. [PubMed: 11316557]
36. Tofts P, Brix G, Buckley D, et al. Estimating kinetic parameters from dynamic contrast-enhanced t 1-weighted MRI of a diffusable tracer: Standardized quantities and symbols. Journal of Magnetic Resonance Imaging 1999;10:223–232. [PubMed: 10508281]
37. Naish JH, Kershaw LE, Buckley DL, et al. Modeling of Contrast Agent Kinetics in the Lung Using T1-Weighted Dynamic Contrast-Enhanced MRI. Magnetic Resonance in Medicine 2009;61:1507–1514. [PubMed: 19319896]
38. Schaefer JF, Vollmar J, Schick F, et al. Solitary Pulmonary Nodules: Dynamic Contrast-Enhanced MR Imaging - Perfusion Differences in Malignant and Benign Lesions. Radiology 2004;232:544–553. [PubMed: 15215548]
39. Lin W, Guo J, Rosen MA, et al. Respiratory motion-compensated radial dynamic contrast-enhanced (DCE)-MRI of chest and abdominal lesions. Magnetic Resonance in Medicine 2008;60:1135–1146. [PubMed: 18956465]
40. Zhang M, Kono M. Solitary Pulmonary Nodules: Evaluation of Blood Flow Patterns with Dynamic CT. Radiology 1997;205:471–478. [PubMed: 9356631]
41. Ma SH, Le HB, Jia BH, et al. Peripheral pulmonary nodules: Relationship between multi-slice spiral CT perfusion imaging and tumor angiogenesis and VEGF expression. BMC Cancer 2008;8:186. [PubMed: 18590539]
42. Pauls S, Mottaghy FM, Schmidt SA, et al. Evaluation of lung tumor perfusion by dynamic contrast-enhanced MRI. Magnetic Resonance Imaging 2008;26:1334–1341. [PubMed: 18538522]

43. Chen X, Park R, Tohme M, et al. MicroPET and autoradiographic imaging of breast cancer alpha v-integrin expression using 18F- and 64Cu-labeled RGD peptide. Bioconjugate Chemistry 2004;15:41–49. [PubMed: 14733582]
44. Beer AJ, Haubner R, Sarbia M, et al. Positron emission tomography using [18F]Galacto-RGD identifies the level of integrin alpha(v)beta3 expression in man. Clinical Cancer Research 2006;12:3942–3949. [PubMed: 16818691]
45. Beer AJ, Lorenzen S, Metz S, et al. Comparison of Integrin aVb3 expression and glucose metabolism in primary and metastatic lesions in cancer patients: a PET study using 18F-galacto-RGD and 18F-FDG. Journal of Nuclear Medicine 2008;49:22–29. [PubMed: 18077538]
46. Morrison MS, Ricketts SA, Barnett J, et al. Use of a novel Arg-Gly-Asp radioligand, 18F-AH111585, to determine changes in tumor vascularity after antitumor therapy. Journal of Nuclear Medicine 2009;50:116–122. [PubMed: 19091899]
47. Evans SM, Joiner B, Jenkins WT, et al. Identification of hypoxia in cells and tissues of epigastric 9L rat glioma using EF5 [2-(2-nitro-1*H*-imidazol-1-yl)-*N*-(2,2,3,3,3-pentafluoropropyl) acetamide]. British Journal of Cancer 1995;72:875–882. [PubMed: 7547234]
48. Raleigh JA, Chou SC, Arteel GE, et al. Comparisons among Pimonidazole Binding, Oxygen Electrode Measurements, and Radiation Response in C3H Mouse Tumors. Radiation Research 1999;151:580–589. [PubMed: 10319731]
49. Rasey JS, Koh WJ, Grierson JR, et al. Radiolabelled fluoromisonidazole as an imaging agent for tumor hypoxia. Int J Radiat Oncol Biol Phys 1989;17:985–991. [PubMed: 2808061]
50. Piert M, Machulla HJ, Picchio M, et al. Hypoxia-specific tumor imaging with 18F-fluoroazomycin arabinoside. Journal of Nuclear Medicine 2005;46:106–113. [PubMed: 15632040]
51. Ziemer LS, Evans SM, Kachur AV, et al. Noninvasive imaging of tumor hypoxia in rats using the 2-nitroimidazole 18F-EF5. European journal of nuclear medicine 2003;30:259–266. [PubMed: 12552344]
52. Lewis JS, McCarthy DW, McCarthy TJ, et al. Evaluation of ^{64}Cu-ATSM In Vitro and In Vivo in a Hypoxic Tumor Model. Journal of Nuclear Medicine 1999;40:177–183. [PubMed: 9935074]
53. Chapman JD, Engelhardt EL, Stobbe CC, et al. Measuring hypoxia and predicting tumor radioresistance with nuclear medicine assays. Radiotherapy and Oncology 1998;46:229–237. [PubMed: 9572615]
54. Zhang X, Melo T, Ballinger JR, et al. Studies of 99mTc-BnAO (HL-91): A non-nitroaromatic compound for hypoxic cell detection. Int J Radiat Oncol Biol Phys 1998;42:737–740. [PubMed: 9845087]
55. Rasey JS, Wui-Jin K, Evans ML, et al. Quantifying regional hypoxia in human tumors with positron emission tomography of [18F]fluoromisonidazole: a pretherapy study of 37 patients. Int J Radiat Oncol Biol Phys 1996;36:417–428. [PubMed: 8892467]
56. Cherk M, Foo S, Poon A, et al. Lack of Correlation of Hypoxic Cell Fraction and Angiogenesis with Glucose Metabolic Rate in Non-Small Cell Lung Cancer Assessed by 18F-Fluoromisonidazole and 18F-FDG PET. Journal of Nuclear Medicine 2006;47:1921. [PubMed: 17138734]
57. Dehdashti F, Mintun MA, Lewis JS, et al. In vivo assessment of tumor hypoxia in lung cancer with 60Cu-ATSM. European Journal of Nuclear Medicine and Molecular Imaging 2003;30:844–850. [PubMed: 12692685]
58. Koh WJ, Bergman KS, Rasey JS, et al. Evaluation of oxygenation status during fractionated radiotherapy in human nonsmall cell lung cancers using [F18]fluoromisonidazole positron emission tomography. Int J Radiat Oncol Biol Phys 1995;33:391–398. [PubMed: 7673026]
59. Koch CJ, Kruuv J, Frey HE. Variation in radiation response of mammalian cells as a function of oxygen tension. Radiation Research 1973;53:33–42. [PubMed: 4734388]
60. Moeller BJ, Dreher MR, Rabbani ZN, et al. Pleiotropic effects of HIF-1 blockade on tumor radiosensitivity. Cancer Cell 2005;8:99–110. [PubMed: 16098463]
61. Schwartz DL, Powis G, Thitai-Kumar A, et al. The selective hypoxia inducible factor-1 inhibitor PX-478 provides in vivo radiosensitization through tumor stromal effects. Mol Cancer Ther 2009;8:947–58. [PubMed: 19372568]

62. Zeng L, Ou G, Itasaka S, et al. TS-1 enhances the effect of radiotherapy by suppressing radiation-induced hypoxia-inducible factor-1 activation and inducing endothelial cell apoptosis. Cancer Sci 2008;99:2327–35. [PubMed: 18823375]
63. Kowanetz M, Ferrara N. Vascular endothelial growth factor signaling pathways: therapeutic perspective. Clin Cancer Res 2006;12:5018–22. [PubMed: 16951216]
64. Nagy JA, Benjamin L, Zeng H, et al. Vascular permeability, vascular hyperpermeability and angiogenesis. Angiogenesis 2008;11:109–19. [PubMed: 18293091]
65. Gorski DH, Beckett MA, Jaskowiak NT, et al. Blockage of the vascular endothelial growth factor stress response increases the antitumor effects of ionizing radiation. Cancer Res 1999;59:3374–8. [PubMed: 10416597]
66. Williams KJ, Telfer BA, Shannon AM, et al. Combining radiotherapy with AZD2171, a potent inhibitor of vascular endothelial growth factor signaling: pathophysiologic effects and therapeutic benefit. Mol Cancer Ther 2007;6:599–606. [PubMed: 17308057]
67. Williams KJ, Telfer BA, Brave S, et al. ZD6474, a potent inhibitor of vascular endothelial growth factor signaling, combined with radiotherapy: schedule-dependent enhancement of antitumor activity. Clin Cancer Res 2004;10:8587–93. [PubMed: 15623642]
68. Jain RK. Normalization of tumor vasculature: an emerging concept in antiangiogenic therapy. Science 2005;307:58–62. [PubMed: 15637262]
69. Winkler F, Kozin SV, Tong RT, et al. Kinetics of vascular normalization by VEGFR2 blockade governs brain tumor response to radiation: role of oxygenation, angiopoietin-1, and matrix metalloproteinases. Cancer Cell 2004;6:553–63. [PubMed: 15607960]
70. Horsman MR, Siemann DW. Pathophysiologic effects of vascular-targeting agents and the implications for combination with conventional therapies. Cancer Res 2006;66:11520–39. [PubMed: 17178843]
71. Dutta PR, Maity A. Cellular responses to EGFR inhibitors and their relevance to cancer therapy. Cancer Lett 2007;254:165–77. [PubMed: 17367921]
72. Raben D, Helfrich B, Chan DC, et al. The effects of cetuximab alone and in combination with radiation and/or chemotherapy in lung cancer. Clin Cancer Res 2005;11:795–805. [PubMed: 15701870]
73. Chinnaiyan P, Huang S, Vallabhaneni G, et al. Mechanisms of enhanced radiation response following epidermal growth factor receptor signaling inhibition by erlotinib (Tarceva). Cancer Res 2005;65:3328–35. [PubMed: 15833866]
74. Bonner JA, Harari PM, Giralt J, et al. Radiotherapy plus cetuximab for squamous-cell carcinoma of the head and neck. N Engl J Med 2006;354:567–78. [PubMed: 16467544]
75. Pore N, Jiang Z, Gupta A, et al. EGFR tyrosine kinase inhibitors decrease VEGF expression by both hypoxia-inducible factor (HIF)-1-independent and HIF-1-dependent mechanisms. Cancer Res 2006;66:3197–204. [PubMed: 16540671]
76. Cerniglia GJ, Pore N, Tsai JH, et al. Epidermal growth factor receptor inhibition modulates the microenvironment by vascular normalization to improve chemotherapy and radiotherapy efficacy. PLoS One 2009;4:e6539. [PubMed: 19657384]
77. Yuan TL, Cantley LC. PI3K pathway alterations in cancer: variations on a theme. Oncogene 2008;27:5497–510. [PubMed: 18794884]
78. Gupta AK, Soto DE, Feldman MD, et al. Signaling pathways in NSCLC as a predictor of outcome and response to therapy. Lung 2004;182:151–62. [PubMed: 15526754]
79. Lee SH, Kim HS, Park WS, et al. Non-small cell lung cancers frequently express phosphorylated Akt; an immunohistochemical study. Apmis 2002;110:587–92. [PubMed: 12390418]
80. Kim IA, Bae SS, Fernandes A, et al. Selective inhibition of Ras, phosphoinositide 3 kinase, and Akt isoforms increases the radiosensitivity of human carcinoma cell lines. Cancer Res 2005;65:7902–10. [PubMed: 16140961]
81. Prevo R, Deutsch E, Sampson O, et al. Class I PI3 kinase inhibition by the pyridinylfuranopyrimidine inhibitor PI-103 enhances tumor radiosensitivity. Cancer Res 2008;68:5915–23. [PubMed: 18632646]
82. Qayum N, Muschel RJ, Im JH, et al. Tumor vascular changes mediated by inhibition of oncogenic signaling. Cancer Res 2009;69:6347–54. [PubMed: 19622766]

83. Gupta AK, Cerniglia GJ, Mick R, et al. HIV protease inhibitors block Akt signaling and radiosensitize tumor cells both in vitro and in vivo. Cancer Res 2005;65:8256–65. [PubMed: 16166302]
84. Jiang W, Mikochik PJ, Ra JH, et al. HIV protease inhibitor nelfinavir inhibits growth of human melanoma cells by induction of cell cycle arrest. Cancer Res 2007;67:1221–7. [PubMed: 17283158]
85. Pore N, Gupta AK, Cerniglia GJ, et al. Nelfinavir down-regulates hypoxia-inducible factor 1alpha and VEGF expression and increases tumor oxygenation: implications for radiotherapy. Cancer Res 2006;66:9252–9. [PubMed: 16982770]
86. Giatromanolaki A, Koukourakis MI, Sivridis E, et al. Relation of hypoxia inducible factor 1 alpha and 2 alpha in operable non-small cell lung cancer to angiogenic/molecular profile of tumours and survival. Br J Cancer 2001;85:881–90. [PubMed: 11556841]
87. Swinson DE, Jones JL, Cox G, et al. Hypoxia-inducible factor-1 alpha in non small cell lung cancer: relation to growth factor, protease and apoptosis pathways. Int J Cancer 2004;111:43–50. [PubMed: 15185341]
88. Kim SJ, Rabbani ZN, Dewhirst MW, et al. Expression of HIF-1alpha, CA IX, VEGF, and MMP-9 in surgically resected non-small cell lung cancer. Lung Cancer. 2005
89. Giatromanolaki A, Koukourakis MI, Sivridis E, et al. Expression of hypoxia-inducible carbonic anhydrase-9 relates to angiogenic pathways and independently to poor outcome in non-small cell lung cancer. Cancer Res 2001;61:7992–8. [PubMed: 11691824]
90. Kon-no H, Ishii G, Nagai K, et al. Carbonic anhydrase IX expression is associated with tumor progression and a poor prognosis of lung adenocarcinoma. Lung Cancer 2006;54:409–18. [PubMed: 17030461]
91. Simi L, Venturini G, Malentacchi F, et al. Quantitative analysis of carbonic anhydrase IX mRNA in human non-small cell lung cancer. Lung Cancer 2006;52:59–66. [PubMed: 16513206]
92. Swinson DE, Jones JL, Richardson D, et al. Carbonic anhydrase IX expression, a novel surrogate marker of tumor hypoxia, is associated with a poor prognosis in non-small-cell lung cancer. J Clin Oncol 2003;21:473–82. [PubMed: 12560438]
93. Malentacchi F, Simi L, Nannelli C, et al. Alternative splicing variants of carbonic anhydrase IX in human non-small cell lung cancer. Lung Cancer 2009;64:271–6. [PubMed: 19022520]
94. Minami K, Saito Y, Imamura H, et al. Prognostic significance of p53, Ki-67, VEGF and Glut-1 in resected stage I adenocarcinoma of the lung. Lung Cancer 2002;38:51–7. [PubMed: 12367793]
95. Nguyen XC, Lee WW, Chung JH, et al. FDG uptake, glucose transporter type 1, and Ki-67 expressions in non-small-cell lung cancer: correlations and prognostic values. Eur J Radiol 2007;62:214–9. [PubMed: 17239556]

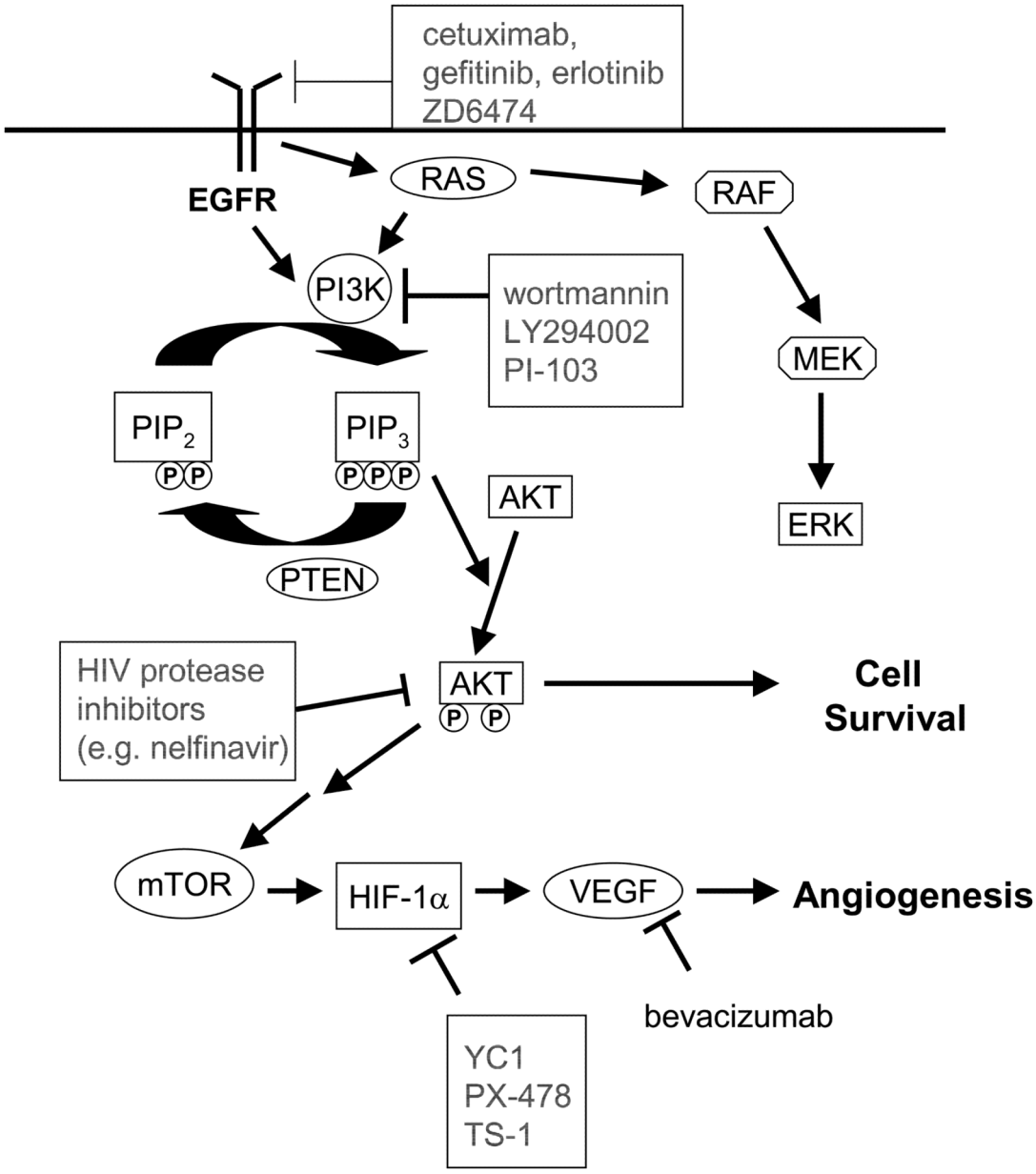

Figure 1. Signal transduction pathways in non-small cell lung cancer

Epidermal growth factor receptor (EGFR) activation, which often occurs in NSCLC, leads to upregulation of the PI3K/Akt pathway as well as the Raf/MEK/ERk kinase pathway. Akt pathway activation has been implicated in both resistance of cells to radiation-induced killing and in increased expression of hypoxia-inducible factor-1 (HIF-1) and vascular endothelial growth factor (VEGF). A number of drugs that can inhibit various points along these pathways have been shown in pre-clinical models to increase the radiation responsiveness of tumors.

Table 1

Significance of HIF-1, CA IX & Glut-1 endogenous hypoxia markers for non-small cell lung cancers

Authors	Hypoxia Markers	# Pts	Treatment	Survival
Giatromanolaki[86]	HIF-1α, HIF-2α, VEGF	98	S	OS for HIF-2α only (Multivariate)
Swinson[87]	HIF-1α	172	S ± RT ± C	OS for CA IX only (Multivariate)
Kim[88]	HIF-1α, CA IX	74 Stage I–II	S	DFS for CA IX Only (Multivariate)
Giatromanolaki[89]	CAIX, HIF-1α, HIF-2α	107	S	OS (Multivariate)
Kon-No[90]	CA IX	134	S	OS, DFS (Univariate only, not multivariate)
Simi L [91]	CA IX mRNA			
Swinson[92]	CA IX	175	S	OS for perinuclear staining pattern (Multivariate)
Malentacchi [93]	CAIX mRNA	101	S	OS for full length CAIX but not for truncated splice form (multivariate)
Nakao [10]	CAIX in stromal fibroblast vs cancer	158	S	OS for stromal fibroblasts but not cancer cells (Multivariate)
Minami[94]	Glut-1	47	S	OS (Multivariate)
Nguyen[95]	Glut-1	53	S ± R ± C	No significance for DFS

Pt: patients; S: Surgery; RT: radiotherapy; C: chemotherapy; Tam: Tamoxifen; ARCON: Carbogen and nicotidamide; CHART: Continuous hyperfractionated accelerated radiotherapy

OC: Oral cavity cancer; NPC: Nasopharyngeal carcinoma; HP: Hypopharyngeal carcinoma; LN+: Lymph node positive;

LRC: locoregional control; DFS: disease-free survival; PFS: Progression-free survival: OS: Overall survival; CSS: Cancer specific suvival; LPFS: Local progression-free survival; MFS: Metastasis-free survival; FFR: Freedom from relapse